Available online at www.sciencedirect.com

ScienceDirect

Mendeleev Commun., 2020, **30**, 211–213

Mendeleev Communications

Albumin aggregation promoted by protoporphyrin *in vitro*

Natalya Sh. Lebedeva, Elena S. Yurina, Yury A. Gubarev,* Aleksey N. Kiselev and Sergey A. Syrbu

G. A. Krestov Institute of Solution Chemistry, Russian Academy of Sciences, 153045 Ivanovo, Russian Federation. E-mail: yury.gu@gmail.com

DOI: 10.1016/j.mencom.2020.03.027

Protoporphyrin upon its binding with serum albumin changes its secondary structure due to the conversion of part of α helices into β-folding. This process results in the association of albumin globules *in vitro*.

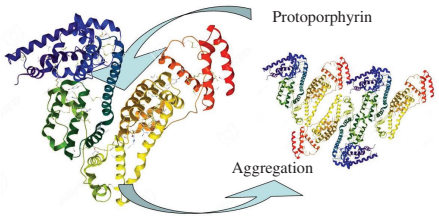

Keywords: porphyrin, albumin, aggregation, UV-VIS spectroscopy, IR spectroscopy, fluorescence.

Protoporphyrin belongs to the blood group porphyrins and its complex with Fe^{2+} called hemin represents a prosthetic group for a number of proteins including those involved in transport and storage of oxygen (*e.g.* hemoglobin, myoglobin), electron transfer, drug and steroid metabolism (*e.g.* cytochromes) as well as signal transduction (*e.g.* nitric oxide synthase, guanylate cyclase). The content of protein-free hemin in a body is controlled by hemoxygenase.[1] Lack of heme or problems in the synthesis of protoporphyrin result in severe diseases such as anemia and porphyria.[2] For their treatment, drugs containing synthetic hemin[3,4] are typically used. On the other hand, an excess of protein-free porphyrin also leads to various pathologies, including temporary thrombosis, liver failure and hemorrhagic diathesis.[5,6] Moreover, an excessive amount of hemin may cause lysis of erythrocyte membranes especially in sickle-shape cell anemia,[7] oxidation of low-density lipoproteins[8] and formation of fatty acid hydroperoxides. These processes lead to renal failure associated with intravascular hemolysis, hemorrhagic damage of the central nervous system and atherogenesis.[8] Localization as well as concentration of protoporphyrin and heme should be strictly regulated in an organism, since any deviation from their optimal amount causes a pathological condition. In turn, the porphyrin content is influenced by the effectiveness of enzymes catabolizing heme as well as by the efficiency of transport systems that ensure the circulation of hydrophobic porphyrin in cells, intercellular fluid and bloodstream. Some systems for the heme and protoporphyrin transportation in mammals have been discovered and extensively explored.

The data on the transport proteins causing the passage of tetrapyrrole macroheterocyclic compounds through the cell membrane, such as HCP1 proteins, FLVCR, Abcg2 and Abcb6, as well as of extracellular heme-binding proteins, such as hemopexin, haptoglobin and serum albumin, is summarized in the review.[9] According to the results of our works[10–12] on the interaction of exogenous synthetic macroheterocyclic compounds with serum albumin, it was hypothesized that the interaction of endogenous porphyrins with albumin can lead to the protein aggregation. This work was aimed at the experimental verification of the hypothesis about the protein aggregation mechanism. The acquired results can afford a detection of the molecular-level reason for β-folding of globular proteins, which is an 'identity card' for diseases like amyloidosis and hypoalbuminemia.[13]

The investigation of the interaction of hydrophobic protoporphyrin **1** with BSA† was carried out in a medium containing 0.5 M NaCl with DMF added to the concentration not exceeding 0.19 M. The synthesis of protoporphyrin **1** is shown in Scheme 1. The chosen concentration of NaCl eliminated the effect of polyelectrolyte protein swelling, while DMF provided the solubility

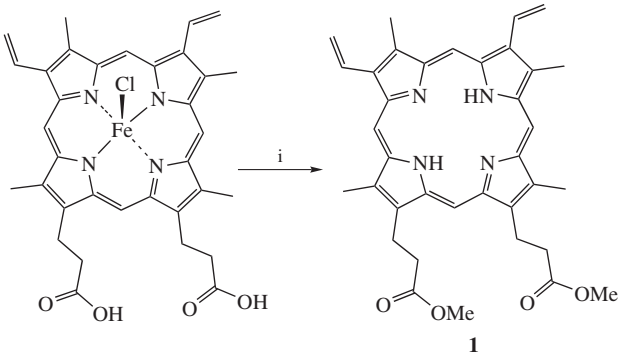

1

Scheme 1 *Reagents and conditions*: i, MeOH, pyridine, CH_2Cl_2, Mohr's salt, AcCl.

† Bovine serum albumin, fraction V (BSA) was purchased from Acros Organics (USA).

Protoporphyrin IX dimethyl ester **1**. Hemin (5.0 g, 7.6 mmol) and pyridine (5.0 ml) were placed in a three-necked flask, then MeOH (300 ml), CH_2Cl_2 (300 ml) and Mohr's salt (20.0 g, 51 mmol) were added. Acetyl chloride (150 ml, 2.1 mol) was gradually added under stirring and cooling, while the temperature was kept below 35 °C. The mixture was stirred for 1 h and then diluted with H_2O (500 ml). The bottom organic layer was separated, washed with aqueous ammonia (25%, 50 ml), then with H_2O (200 ml) and dried over anhydrous Na_2SO_4. The product was purified by chromatography on silica gel 60 mesh using CH_2Cl_2 as the eluent. Yield 4.48 g (99%).

UV-VIS and fluorescence spectra were recorded using an AvaSpec-2048 spectrophotometer (Avantes, Netherlands) at 25°C. A monochromatic LED UVTOP-295 (Sensor Electronic Technology, USA) was employed as an excitation light source in the fluorescence experiments. IR spectra were recorded on an Avatar 360 IR-Fourier spectrometer (Thermo Nicolet, USA) in KBr pellets.

© 2020 Mendeleev Communications. Published by ELSEVIER B.V. on behalf of the N. D. Zelinsky Institute of Organic Chemistry of the Russian Academy of Sciences.

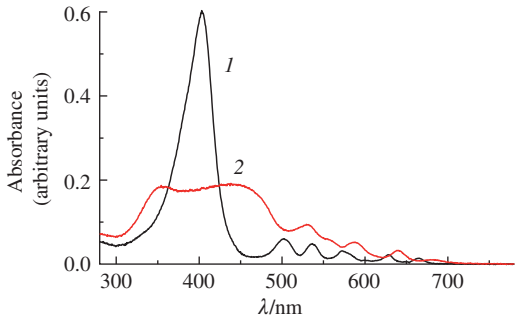

Figure 1 UV-VIS spectra of protoporphyrin **1** solutions in (*1*) DMF (9.3×10^{-6} M) and (*2*) aqueous DMF (0.19 M).

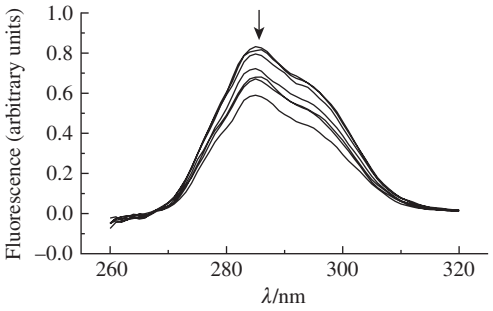

Figure 3 Synchronous fluorescence spectra of tyrosine recorded during BSA titration by protoporphyrin **1**.

of compound **1** and did not affect the protein secondary structure under these conditions. The BSA concentration in the working solutions was 0.08%, the protein existed in a monomeric state, which was confirmed by our previous hydrodynamic data[14] and by the results of dynamic light scattering, according to which the hydrodynamic diameter of the BSA globule was 9.8 nm (100%). This diameter is consistent with the known data[15–17] on the protein in its native state and monomeric form.

According to the electronic absorption spectra, protoporphyrin **1** in an aqueous organic solvent exists in an associated state, since the absorption bands in its UV-VIS spectrum are bathochromically shifted and broadened (Figure 1).

Titration of protoporphyrin **1** with BSA resulted in shifting the associated equilibrium towards porphyrin monomerization as evidenced by the electronic spectroscopy data. Retitration of the protein with porphyrin caused a decrease in BSA fluorescence (λ_{ex} = 295 nm) originated from tryptophan residues at the 134 and 213 positions of polypeptide chain located in IIA and IB subdomains of the protein. Note, that the quenching was not complete (Figure 2).

This suggests that the protoporphyrin 1 is locatized in such a manner that only one of the two tryptophan fluorophores is quenched, or the quencher and the fluorophores are distant from each other. Probably, protoporphyrin is localized similarly to its iron complex in the heme site FA1,[18] *viz.* in the D-shaped cavity in the centre of four-helix bundle of the BSA subdomain IB,[19] and the π–π interaction of aromatic residues Tyr138 and Tyr161 with porphyrin π-system occurs. The HOOC–CH_2–CH_2 substituents at the porphyrin macrocycle are known to be located at the interface between the I and III domains and stabilized by electrostatic and H-binding interactions with the Arg114, His146 and Lys190 residues.[12,19,20] The central metal ion of the protoporphyrin complex contributes as well to the stabilization of associate with the protein through a coordination bond with the Tyr161 oxygen atom. In this arrangement, only the Trp134 residue near the D-shaped cavity can participate in the fluorescence quenching, while the Trp213 residue is sterically inaccessible to heme. Fe^{III} protoporphyrin reported[19,20] and protoporphyrin **1** represent structural analogues, the difference between them being in the reaction centre, namely complexing metal *vs.* two pyrrole protons, and also in carboxylic groups *vs.* methyl esters in peripheral protoporphyrin substituents.

The localization of protoporphyrin **1** in the BSA globule can be clarified by comparison of the contributions to quenching for tyrosine (λ_{ex} = 280 nm) and tryptophan residues (λ_{ex} = 295 nm), as well as from the synchronous fluorescence. Figures 2–5 demonstrate the fluorescence of protein and its complexes with compound **1**. The protein fluorescence quenching upon excitation at 280 nm was about 46% for the BSA : porphyrin molar ratio of 1 : 0.8. The fluorescence quenching at λ_{ex} = 295 nm was 31%. The acquired data allows us to conclude that the quencher causes a greater effect on tryptophan residues than on tyrosine ones. Probably, protoporphyrin **1** is not located in the D-shaped cavity in the centre of four-helix bundle of IB subdomain,[19] and is arranged similar to heme in the IB subdomain. The synhronous spectra provide some additional information on the molecular microenvironment of the fluorophores. These spectra for BSA and its complex with protoporphyrin **1** were recorded using $\Delta\lambda$ = 60 and 15 nm, respectively, to estimate the contribution from quenching fluorescence of tryptophan and tyrosine. An increase in the concentration of porphyrin in the considered systems resulted in a decrease in the intensity and a slight hypsochromic shift of the fluorescence bands. In addition, the changes in fluorescence associated with the presence of tryptophan residues in BSA led to distorsion of spectrum, namely the inversion of emission intensity at 270 and 288 nm. These changes in the synchronous spectra are typically interpreted as alterations in the microenvironment of the protein fluorophore upon its interaction with a quencher.[21–23] Thus, the acquired data suggests a change in the secondary structure of BSA as a result of its binding with protoporphyrin **1**.

IR spectroscopy allowed us to obtain a reliable information on the conformational alternations in the protein globule, caused by the interaction with protoporphyrin. Figure 6 shows IR spectra for the I and the III amide regions of BSA. The second amide region (1400–1580 cm^{-1}) is not considered, since a very intense absorption of protoporphyrin occurs in this range and the interpretation of BSA binding of with porphyrin is fairly difficult.

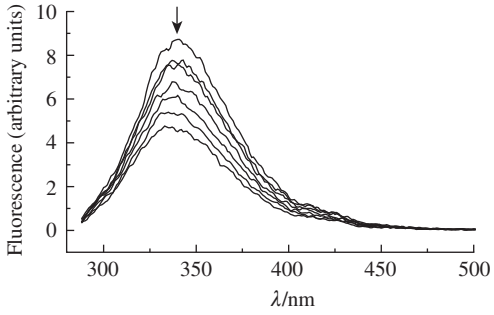

Figure 2 Fluorescence spectra of BSA titrated by protoporphyrin **1** using λ_{ex} = 280 nm.

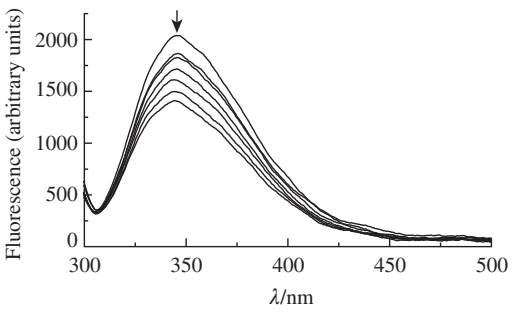

Figure 4 Fluorescence spectra of BSA titrated by protoporphyrin **1** using λ_{ex} = 295 nm.

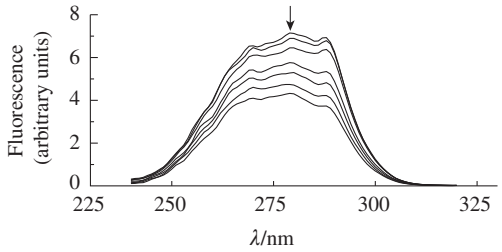

Figure 5 Synchronous fluorescence spectra of tryptophan recorded during the BSA titration by protoporphyrin **1**.

As one can see from the acquired data, the I and the III amide regions (see Figure 6, line *2*) are typical of the protein in its native form. The main peak at ~1655 cm^{-1} is present in the spectrum, suggesting that alpha structuring is preserved and dominates over the other elements of secondary structure.

The III amide region in the IR spectrum of BSA contains vibration bands at ~1314 and 1243 cm^{-1} (see Figure 6, line *2*), falling within the characteristic range for α-helices (1330–1290 cm^{-1}) and an arbitrary helix (1250–1220 cm^{-1}). At the same time, no pronounced peaks were recorded in the area responsible for the β-folding (1290–1260 cm^{-1}), which is consistent with the known IR data for albumin[24–26] in its native conformation, where the main type of albumin secondary structure has been represented by α-helix constituting at least 67% and by the disordered fragments for the remaining 23%.

The interaction with protoporphyrin **1** causes changes in the position of vibration bands. The main band in the I amide region is broadened for porphyrin bound to protein and the peaks appear at ~1650, 1629 and 1618 cm^{-1}. It would not be correct to interpret these changes as dealing with alterations in the protein secondary structure, since compound **1** absorbs in the region of 1626 cm^{-1} (see Figure 6, line *1*).[27]

More informative is the III amide region, wherein a shift in the absorption band of BSA at 1319 cm^{-1} to 1314 cm^{-1} is observed. The intensity of absorption at 1243 cm^{-1} decreases and a pronounced peak emerges at ~1252 cm^{-1}. Its appearance indicates the transition from a disordered to the β-folded structure. In addition, weak bands that are not represented in the spectra of BSA and porphyrin arise in the regions of 1290, 1284 and 1278 cm^{-1}, indicating the formation of β-folded moieties in the protein. The acquired data supports the synchronous fluorescence results concerning a change in the BSA secondary structure due to the β-folding as a result of binding. It is known that the β-folding of globular proteins represents the first step in the formation of amyloid protein structures as an origin of many pathologies.[28]

The aggregation state of BSA in solution was evaluated using dynamic light scattering, which revealed that large associates and aggregates possessing a hydrodynamic diameter of 154 nm (92%) and 4871 nm (2%) were formed in the solutions investigated, and a part of the protein globules remained unassociated and retained the original diameter of 9.62 (8%). Probably, protoporphyrin **1** during intercalation into the BSA globule causes a change in the secondary structure of protein. This leads to the exposure of hydrophobic regions of the polypeptide chain to the surface of the globule. Moreover, this phenomenon has a local character, since the most of protein is α-structured, and results in the aggregation of protein globules.

In conclusion, the acquired data allowed us to confirm that an excess of free porphyrin can result in the aggregation of albumin and, therefore, such conditions as amyloidosis and hypoalbuminemia.

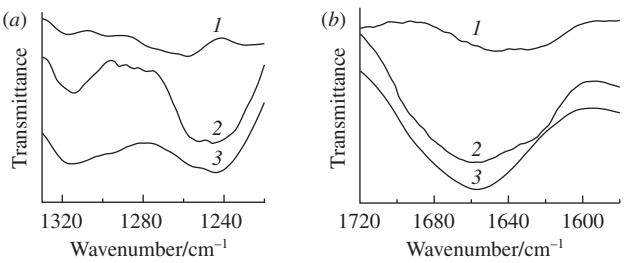

Figure 6 IR spectra recorded for (*a*) I amide region and (*b*) III amide region of (*1*) protoporphyrin **1**, (2) protoporphyrin **1**–BSA complex and (*3*) BSA.

This work was supported by the Russian Foundation for Basic Research (grant no. 19-03-00468). The authors are grateful to The Upper Volga Region Centre of Physicochemical Research for the analysis of samples.

References

1 M. Makarska-Bialokoz, *Spectrochim. Acta, Part A*, 2018, **193**, 23.
2 D. Chiabrando, S. Mercurio and E. Tolosano, *Haematologica*, 2014, **99**, 973.
3 J. Chung, C. Chen and B. H. Paw, *Curr. Opin. Hematol.*, 2012, **19**, 156.
4 M. Balwani and R. J. Desnick, *Hematology, ASH Education Program.*, 2012, 19.
5 Y. I. Miller and N. Shaklai, *Biochem. Mol. Biol. Int.*, 1994, **34**, 1121.
6 D. J. Schaer, P. W. Buehler, A. I. Alayash, J. D. Belcher and G. M. Vercellotti, *Blood*, 2013, **121**, 1276.
7 T. H. Schmitt, W. A. Frezzatti and S. Schreier, *Arch. Biochem. Biophys.*, 1993, **307**, 96.
8 V. Jeney, J. Balla, A. Yachie, Z. Varga, G. M. Vercellotti, J. W. Eaton and G. Balla, *Blood*, 2002, **100**, 879.
9 P. Krishnamurthy, T. Xie and J. D. Schuetz, *Pharmacol. Ther.*, 2007, **114**, 345.
10 N. Sh. Lebedeva, E. S. Yurina, Y. A. Gubarev and S. A. Syrbu, *J. Mol. Liq.*, 2019, **288**, 111024.
11 N. Sh. Lebedeva, E. S. Yurina, S. S. Guseinov, Y. A. Gubarev and S. A. Syrbu, *Dyes Pigm.*, 2019, **162**, 266.
12 N. Sh. Lebedeva, E. S. Yurina, Yu. A. Gubarev, S. A. Syrbu and N. L. Pechnikova, *Mendeleev Commun.*, 2018, **28**, 158.
13 M. K. Siddiqi, P. Alam, S. K. Chaturvedi, Y. E. Shahein and R. H. Khan, *Front. Biosci., Elite Ed.*, 2017, **9**, 1.
14 N. Sh. Lebedeva, Y. A. Gubarev, A. I. Vyugin and O. I. Koifman, *J. Lumin.*, 2015, **166**, 71.
15 W. Lei, G. Jiang, Q. Zhou, B. Zhang and X. Wang, *Phys. Chem. Chem. Phys.*, 2010, **12**, 13255.
16 V. S. Jisha, K. T. Arun, M. Hariharan and D. Ramaiah, *J. Am. Chem. Soc.*, 2006, **128**, 6024.
17 D. Hu, Z. Sheng, G. Gao, F. Siu, C. Liu, Q. Wan, P. Gong, H. Zheng, Y. Ma and L. Cai, *Biomaterials*, 2016, **93**, 10.
18 G. Fanali, A. di Masi, V. Trezza, M. Marino, M. Fasano and P. Ascenzi, *Mol. Aspects Med.*, 2012, **33**, 209.
19 P. A. Zunszain, J. Ghuman, T. Komatsu, E. Tsuchida and S. Curry, *BMC Struct. Biol.*, 2003, **3**, 6.
20 M. Wardell, Z. Wang, J. X. Ho, J. Robert, F. Ruker, J. Ruble and D. C. Carter, *Biochem. Biophys. Res. Commun.*, 2002, **291**, 813.
21 M. E. Pacheco and L. Bruzzone, *J. Lumin.*, 2013, **137**, 138.
22 V. Anbazhagan and R. Renganathan, *J. Lumin.*, 2008, **128**, 1454.
23 Y.-J. Hu, Y. Liu, J.-B. Wang, X.-H. Xiao and S.-S. Qu, *J. Pharm. Biomed. Anal.*, 2004, **36**, 915.
24 M. Jackson and H. H. Mantsch, *Crit. Rev. Biochem. Mol. Biol.*, 1995, **30**, 95.
25 E. A. Cooper and K. Knutson, in *Physical Methods to Characterize Pharmaceutical Proteins* (*Pharmaceutical Biotechnology*, vol. 7), eds. J. N. Herron, W. Jiskoot and D. J. A. Crommelin, Springer, 1995, pp. 101–143.
26 S. J. Prestrelski, T. Arakawa and J. F. Carpenter, *Arch. Biochem. Biophys.*, 1993, **303**, 465.
27 L. J. Boucher and J. J. Katz, *J. Am. Chem. Soc.*, 1967, **89**, 1340.
28 D. J. Selkoe, *Nature*, 2003, **426**, 900.

Received: 6th August 2019; Com. 19/6010